Eur. J. Mineral., 33, 221–232, 2021
https://doi.org/10.5194/ejm-33-221-2021

European Journal of Mineralogy
Open Access

A gemmological study of the reliquary crown of Namur, Belgium

Yannick Bruni[1], Frédéric Hatert[1], Philippe George[2], Hélène Cambier[3], and David Strivay[4]

[1]Laboratory of Mineralogy, University of Liège B18, 4000 Liège, Belgium
[2]Liège Treasure of the Cathedral, Rue Bonne Fortune 6, 4000 Liège, Belgium
[3]Musée Diocésain, Cathédrale Saint-Aubain, Place Saint Aubain, 5000 Namur, Belgium
[4]European Centre of Archaeometry, University of Liège B15, 4000 Liège, Belgium

Correspondence: Yannick Bruni (yannick.bruni@uliege.be)

Received: 26 November 2020 – Revised: 16 March 2021 – Accepted: 17 March 2021 – Published: 27 April 2021

Abstract. The reliquary crown, hosted in the diocesan museum of Namur, was produced during the beginning of the 13th century to shelter a fragment of the holy crown of thorns. This beautiful piece of goldsmithery is made of eight gold plates, topped by round lobes, and connected to each other by hinges blocked with a pin decorated by a pearl. The crown is decorated by filigrees, flowers, and approximately 400 pearls and coloured (green, reddish pink, turquoise, red, blue) stones showing simple cutting with various sizes and shapes. Raman and portable X-ray fluorescence spectrometer (pXRF) techniques have been used to determine the nature and sources of all samples, as well as the composition of filigrees. Analyses have identified emeralds from Pakistan, reddish pink spinels from Tajikistan, red almandine garnets from India, turquoise from Iran, blue sapphires from Sri Lanka or Myanmar, and European pearls. The filigrees contain approximately 86 wt % Au, 7 wt % Ag, and 7 wt % Cu, thus confirming a gold-rich composition. The gemstones, contemporary with the crown, probably arrived in Europe by the silk trade road.

1 Introduction

Since the beginning of the 20th century, a reliquary containing a fragment of the holy crown of thorns has been displayed in the diocesan museum of Namur, inside the Saint Aubin cathedral. The reliquary crown is comprised of eight gold plates measuring approximately 7 cm in height, topped by round lobes, and connected to each other by hinges locked with a pin decorated by a pearl (Fig. 1). This structure allows the crown to be easily and quickly dismantled for transportation, restoration, or in case of an emergency event. The eight articulated plates are decorated by gold filigrees, metal flowers, pearls, and blue, turquoise, red, green, and pink gemstones with different sizes and shapes (Figs. 1 and 2). The internal part of the crown is garnished by red velvet (Fig. 1b) (Gaborit-Chopin, 1975; Collet, 2013). The reliquary is classified among the exceptional historic religious items of Wallonia.

The crown from Namur is dated to the beginning of the 13th century. Around 1206, Henri de Flandre-Hainaut, emperor of Constantinople (1206–1212), sent to his brother, Philippe le Noble, count of Namur, two thorns from the original crown of Christ (Salet, 1967; Van Tricht, 2000; Collet, 2013). To shelter them, Philippe ordered the manufacture of a reliquary crown on which were attached, until 1889, two small capsules containing the holy thorns, as well as of its octagonal protective wooden box, decorated with enamelled medallions from the Limousin region (Collet, 2013; Vanrillaer, 2017).

The past decades have seen an increasing interest in the analysis of ancient goldsmith's items by modern archaeometric techniques. Several examples of these studies occur in the literature, such as the Raman and portable X-ray fluorescence spectrometer (pXRF) investigations of the reliquary from Lierneux (Bruni et al., 2020), of the cross from Liège Cathedral (Demaude et al., 2016, 2017), and of the reliquary bust of Saint Lambert (Bruni et al., 2019). To date, the reliquary crown of Namur had never been investigated by these modern archaeometric techniques. The goal of the present

Figure 1. Photographs of the reliquary crown of Namur (© Frédéric Hatert). **(a)** Front view. **(b)** Top view. **(c)** Close up of the p6 gold plate.

paper is consequently to characterize the gemstones decorating the crown by using portable Raman and X-ray fluorescence spectrometric methods. The chemical data obtained from the samples will help us to determine the mineralogical nature of gems and to give some hypothesis concerning their original deposits and the commercial roads used during the 13th century.

2 Materials and methods

The reliquary crown is a precious item that should not be moved lest it be damaged. Numerous pearls and 169 stones, showing different colours, various shapes, and often simple cuttings, decorate its entire surface. The best methods for these archaeometric analyses are therefore Raman and portable X-ray fluorescence spectrometries since they are handheld and non-destructive.

The portable Raman spectrometer used in our analyses is an Enwave Optronics EZRaman-I-DUAL, loaned by the European Centre of Archaeometry of Liège, in Belgium. This optic-fibre-based instrument is equipped with two light sources: a green Nd:YAG laser (532 nm) and a red diode source (785 nm). The spot diameter of the optic fibres is approximately 6 mm, and the detector is of charge-coupled device type (CDD). A removable rubber tip is attached to the end of the probe to protect the beam from ambient light and to always keep a relatively constant sample–probe distance during repeated measurements. The power of the spectrometer can be adjusted to a maximal output power reaching 400 and 100 mW for the 785 and 532 nm radiations, respectively; only 10% of the maximal power was used in our study (10 to 40 mW). The spectral region covered was between 100 and 3200 cm^{-1} for the 785 nm diode and between 100 and 4000 cm^{-1} for the 532 nm laser. Consequently, spectral resolutions are different, namely 7 and 8 cm^{-1} for the 785 and 532 nm sources, respectively. Duration of analysis was of 60 to 120 s. Raman spectra were recorded in the software in txt file format and then exported in Excel. The final spectra were cut at 1400 cm^{-1} (spectral region between 100 and 1400 cm^{-1}) for a better presentation, and they were not affected by any post-acquisition data manipulation. The comparative Raman spectra came from different bibliographic sources (see below).

The portable X-ray fluorescence spectrometer (pXRF) is a Thermo Fisher Niton XL3t, equipped with a "GOLDD" detector, from the Laboratory of Mineralogy of the University of Liège, Belgium. The pXRF was positioned against the glass beads, and X-rays were generated when the nose cone was in direct contact with the surface. X-rays are produced with a silver-anode tube, using an acceleration voltage of 50 kV and a current of 200 µA; the spot size shows a diameter of 3 mm. The lightest detectable element is magnesium, but without a helium flow, this element cannot be detected

with a good accuracy. The standardization mode selected is the "Cu/Zn Mining", which includes all elements of interest for a gemmological study (e.g. Si, Al, P, Mn, Fe). This analysis mode uses successively four separate filters to determine the concentrations in percentage of each chemical element: a high filter (15 s counting time), a main filter (15 s), a low filter (15 s), and a light filter (30 s), leading to a total counting time of 75 s per analysis point. The software utilizes a fundamental parameters algorithm to determine concentrations of each element. The spectra and concentration values obtained from the XLT3 were downloaded to a computer for calculations. The concentration values were multiplied according to a standard element oxide conversion table to produce a percentage by weight (wt %) of each oxide, and then the values were normalized to a total of 100 wt %.

3 Gemstone description and identification

Approximately 400 coloured stones and pearls decorate the reliquary crown of Namur, with more or less 20 gemstones per gold plate, as well as 50 pearls, arranged in two horizontal rows. Larger pearls are also located on the top of the pins maintaining the hinges (Fig. 1; the exact nomenclature and position of the stones and pearls is given in Fig. S1).

The stones show various colours (red, reddish pink, blue, turquoise, and green), shapes (round, hexagonal, rectangular, triangular, and fancy), and sizes (from 5 to 20 mm). The pearls are always white with button to rounded shapes and with diameters from 5 to 15 mm. The main cutting is the cabochon (Figs. 1 and 2), but one big blue sample shows a large table with four small facets (Fig. 1a). Stones and pearls occur in gold settings, either without hooks or rarely with four hooks (Fig. 2e). Inclusions, distinct colour zonings, traces of removed inclusions (Fig. 2b, h), and growth and star structures (Fig. 2c, d) are also sometimes observed.

It was impossible to analyse all samples by Raman spectrometry because some of them show sizes that are too small. Moreover, the high values of fluorescence and absorption in dark coloured stones made the analyses sometimes difficult to obtain. These phenomena are common in portable instrumentation (Jehlička et al., 2011). Some analyses were therefore omitted due to their poor quality. However, many stones of each colour and pearls were analysed with no laser-induced fluorescence except for the turquoises. A list of their Raman bands is available in Table S1.

The green gemstones p1-6 and p5-6 show Raman spectra characterized by a strong peak located between 684 and 686 cm^{-1}, a medium intensity peak at 1068–1070 cm^{-1}, and four weak peaks at 320, 398, 522, and 1010 cm^{-1} (Fig. 3, p1-6). These results are in good agreement with beryl spectra from RRUFF (2020) and Culka and Jehlička (2019). The red stones p3-1, p4-1, p5-3, and p6-3 show spectra with an intense peak at 916 cm^{-1}, as well as six weak peaks at 346, 492, 550, 626, 856, and 1040 cm^{-1} (Fig. 3, p5-3), corresponding to almandine or pyrope-almandine spectra (RRUFF, 2020; Culka and Jehlička, 2019). The spectra of the two blue stones p3-4 and p4-3 contain an intense peak at 414 cm^{-1}, surrounded by weak peaks at 370–374, 640–648 and 740–746 cm^{-1} (Fig. 3, p3-4), in good agreement with the corundum spectra published by Kadleíková et al. (2001). The two reddish pink stones p1-2 and p8-3 show spectra revealing a strong peak located between 402 and 404 cm^{-1}, as well as two less intense peaks at 660–668, and 760–764 cm^{-1} (Fig. 3, p8-3). These spectra are in good agreement with spinel spectra from RRUFF (2020).

Figure 2. Detailed pictures of the gems set in the reliquary crown of Namur (© Frédéric Hatert). **(a)** Rectangular emerald p5-1. **(b)** Rounded red garnet p6-2. **(c)** Sapphire with a growth structure p1-4. **(d)** Sapphire with oriented rutile inclusions producing a partial asterism p3-2. **(e)** Reddish pink spinel p1-3. **(f)** Round pearl between sapphire p8-1 and spinel p8-3. **(g)** Turquoise on the p1 gold plate. **(h)** Rectangular garnet with two traces of removed inclusions p3-3.

Table 1. Chemical composition of gems and pearls decorating the crown of Namur.

Sample	Phase	Colour	BeO / H_2O[1]	MgO[2]	Al_2O_3	SiO_2	P_2O_5	SO_3	ZnO	K_2O	CaO	V_2O_5	Cr_2O_3	TiO_2	MnO	Fe_2O_3[3]	CuO	SrO
P1-4	Sapphire	Blue	–	–	99.50	–	–	–	–	–	–	0.01	0.01	0.08	–	0.40	–	–
P2-2	Sapphire	Blue	–	–	98.37	–	–	–	–	–	–	0.02	0.02	0.27	–	1.33	–	–
P2-5	Sapphire	Blue	–	–	98.99	–	–	–	–	–	–	0.02	0.01	0.12	–	0.85	–	–
P3-2	Sapphire	Blue	–	–	99.32	–	–	–	–	–	0.06	0.01	0.01	0.09	–	0.51	–	–
P3-4	Sapphire	Blue	–	–	99.22	–	–	–	–	–	0.14	0.01	0.01	0.13	–	0.49	–	–
P4-3	Sapphire	Blue	–	–	98.74	–	–	–	–	–	–	0.02	0.02	0.20	–	1.02	–	–
P5-2	Sapphire	Blue	–	–	99.59	–	–	–	–	–	–	0.01	0.01	0.07	–	0.32	–	–
P6-1	Sapphire	Blue	–	–	99.67	–	–	–	–	–	–	0.01	0.01	0.06	–	0.27	–	–
P6-4	Sapphire	Blue	–	–	98.71	–	–	–	–	–	–	0.01	0.02	0.18	–	1.08	–	–
P7-2	Sapphire	Blue	–	–	98.76	–	–	–	–	–	0.21	0.02	0.01	0.14	–	0.85	–	–
P7-3	Sapphire	Blue	–	–	99.14	–	–	–	–	–	–	0.01	0.01	0.11	–	0.73	–	–
P8-1	Sapphire	Blue	–	–	98.74	–	–	–	–	–	0.06	0.01	0.01	0.19	–	1.00	–	–
P8-4	Sapphire	Blue	–	–	98.58	–	–	–	–	–	–	0.01	0.01	0.25	–	1.16	–	–
P7-1	Turquoise	Turquoise	17.72	–	36.83	1.85	32.80	1.23	0.26	–	0.46	–	–	–	–	0.59	8.21	–
P2-3	Garnet	Red	–	7	21.60	35.69	1.01	0.74	–	–	1.90	0.02	0.09	0.06	1.43	30.71	–	–
P2-4	Garnet	Red	–	5	21.55	35.73	0.95	0.96	–	–	1.89	–	0.08	0.03	1.46	32.75	–	–
P3-1	Garnet	Red	–	6	22.57	37.94	0.17	0.13	–	–	1.77	–	0.04	0.05	1.15	29.75	–	–
P3-3	Garnet	Red	–	3	21.07	37.46	0.16	0.28	–	–	2.00	0.03	0.04	0.05	1.71	33.37	–	–
P4-1	Garnet	Red	–	7	19.10	40.56	0.16	0.16	–	–	1.85	–	0.05	0.04	1.32	29.55	–	–
P4-2	Garnet	Red	–	7	22.45	34.61	0.16	0.79	–	–	0.48	–	0.01	0.01	0.29	34.52	–	–
P4-4	Garnet	Red	–	5	18.90	37.05	0.16	0.53	–	–	0.50	–	–	–	0.26	38.02	–	–
P5-3	Garnet	Red	–	4	21.12	36.23	0.17	0.41	–	–	0.69	–	0.01	–	0.21	36.98	–	–
P5-4	Garnet	Red	–	7	19.72	41.89	0.19	0.09	–	–	1.77	0.02	0.02	0.04	1.34	27.83	–	–
P6-2	Garnet	Red	–	4	19.68	30.96	1.15	1.90	–	–	0.90	0.02	0.05	0.01	0.27	40.51	–	–
P6-3	Garnet	Red	–	4	20.77	37.15	0.59	1.45	–	–	1.89	0.04	0.07	0.07	1.61	31.87	–	–
P7-1	Garnet	Red	–	7	23.02	34.07	0.12	0.09	–	–	0.57	0.02	0.01	–	0.36	34.95	–	–
P7-4	Garnet	Red	–	6	23.44	36.09	0.44	0.42	–	–	1.64	0.02	0.10	0.05	1.51	30.61	–	–
P8-5	Garnet	Red	–	7	24.19	35.91	0.17	0.23	–	–	1.27	0.02	0.08	0.06	1.50	29.55	–	–
P1-2	Spinel	Pink	–	26	68.95	1.72	1.04	0.75	0.28	–	0.15	0.28	0.13	–	–	0.90	–	–
P1-3	Spinel	Pink	–	24	73.38	0.19	–	0.33	0.18	0.06	0.12	0.16	0.07	–	–	0.86	–	–
P8-2	Spinel	Pink	–	27	69.16	1.12	0.92	0.91	0.22	–	–	0.15	0.19	–	–	0.82	–	–
P8-3	Spinel	Pink	–	25	69.51	1.72	0.86	1.28	0.26	0.20	0.43	0.11	0.04	–	–	0.63	–	–
P1-1	Emerald	Green	13.96	2	13.53	67.12	0.17	0.33	–	0.10	0.06	0.11	1.60	–	–	0.92	–	–
P1-6	Emerald	Green	13.96	2	13.34	67.22	0.17	0.30	–	0.14	0.20	0.08	1.78	–	–	0.92	–	–
P5-1	Emerald	Green	13.96	1	13.62	67.37	0.14	0.24	–	0.07	0.14	0.04	1.69	–	–	0.85	–	–
P5-6	Emerald	Green	13.96	3	12.45	67.60	0.24	0.38	–	0.20	0.08	0.06	1.31	–	–	0.81	–	–
P6-5	Emerald	Green	13.96	3	12.95	67.19	0.18	0.21	–	0.12	0.05	0.07	1.62	–	–	1.02	–	–
P2-1	Pearl	White	–	–	0.65	0.21	0.22	1.01	0.58	0.15	96.95	–	–	–	0.08	–	–	0.14
P4-5	Pearl	White	–	–	0.69	0.40	1.11	1.50	0.29	0.33	95.49	–	–	–	0.12	–	–	0.06
P5-5	Pearl	White	–	–	0.37	1.65	1.83	1.02	0.15	0.05	94.71	–	–	–	0.14	–	–	0.08
P7-5	Pearl	White	–	–	0.83	0.90	1.29	1.47	0.45	0.10	94.78	–	–	–	0.11	–	–	0.06

Analyses realized by pXRF; data presented as percentage by weight (wt %) of oxides normalized to 100 wt %. The – signifies below detection limit. Percentages above 2 wt % are shown in bold. [1] Calculated values for BeO in emerald and for H_2O in turquoise. [2] MgO amounts are rounded to the unit because this element cannot be measured with more precision. [3] FeO_{total} for emerald and garnet.

The four samples p2-1, p4-5, p5-5, and p7-5 visually look like pearls; their Raman spectra are characterized by an intense peak situated at 1086 cm^{-1}, as well as by three less intense peaks at 158, 202, and 702 cm^{-1} (Fig. 3, p4-5). These results are in good agreement with the spectra of aragonite published by Wehrmeister et al. (2007), Karampelas et al. (2019), and Athavale and Hambarde (2020).

Table 2. Chemical compositions of noble metals constituting the reliquary crown of Namur.

Sample	Ag	Au	Pb	As	Cu	Fe	Ni	Co
M1	**6.53**	**86.01**	–	–	**7.33**	–	0.13	–
M2	**7.57**	**85.38**	–	–	**6.90**	–	0.14	–
M3	**6.65**	**86.22**	–	–	**7.00**	–	0.13	–

Analyses realized by pXRF; data presented as percentage by weight (wt %) of elements normalized to 100 wt %. The – signifies below detection limit. Percentages above 2 wt % are shown in bold.

4 Chemical characterization by portable X-ray fluorescence spectrometry

Chemical analyses of the stones, pearls, and noble metals were performed with a pXRF spectrometer; the results are given in Tables 1 and 2. As for Raman spectroscopy, it was impossible to analyse all samples because their sizes are too small. Some analyses were also omitted due to their poor quality. Magnesium is rounded to the unit because it is the lightest detectable element, so it cannot be measured with more precision. Beryllium and water were not directly measured by pXRF; consequently, their amounts are calculated values.

Green stones show compositions characterized by approximately 65 wt % SiO_2, 15 wt % BeO, and 14 wt % Al_2O_3. Minor amounts of Cr_2O_3 (1 wt %–2 wt %), MgO (2 to 3 wt %), Fe_2O_3 (< 0.99 wt %), and V_2O_5 (< 0.12 wt %) were

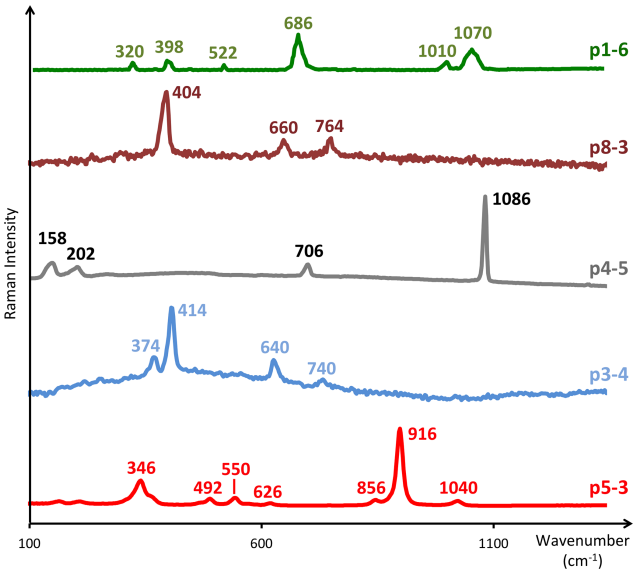

Figure 3. Raman spectra of gemstones from the Crown of Namur: emerald (p1-6), spinel (p8-3), pearl (p4-5), sapphire (p3-4), and almandine (p5-3).

also observed (Table 1). These chemical analyses correspond to emerald compositions, a green variety of beryl ($Be_3Al_2Si_6O_{18}$) whose colour is allochromatic mainly due to the substitution of Al^{3+} by Cr^{3+} at the Y octahedral site (Fritsch and Rossman, 1987; Ferreira de Araújo Neto et al., 2019). Vanadium may also produce a green colour in beryl, but such green beryls are not considered as true emeralds by a majority of gemmologists (Fritsch and Rossman, 1987; Ferreira de Araújo Neto et al., 2019).

Red samples contain 34 wt %–42 wt % SiO_2, 30 wt %–40 wt % FeO, 19 wt %–24 wt % Al_2O_3, and 3 wt %–7 wt % MgO, with small amounts of CaO (0.46 wt %–2.00 wt %) and MnO (0.21 wt %–1.61 wt %) (Table 1). These compositions are similar to those of almandine garnet ($Fe_3Al_2Si_3O_{12}$) with a low content of pyrope (Mg_3Al_2) and spessartine (Mn_3Al_2). Divalent iron, located on the distorted 8-coordinated cubic site of the structure, is responsible for the idiochromatic dark red colour of this garnet (Fritsch and Rossman, 1987).

Concerning blue stones, the pXRF reveals contents of Al_2O_3 very close to 100.00 wt %. Minor amounts of iron (< 1.16 wt %) and titanium (< 0.25 wt %) were also observed in all samples (Table 1). These gemstones consequently correspond to sapphire, a variety of corundum (Al_2O_3) whose blue colour is allochromatic, caused by the inter-valence charge transfer Fe^{2+}-O-Ti^{4+} (Fritsch and Rossman, 1988).

The analyses of reddish pink gemstones reveal a high level of MgO and Al_2O_3, reaching 27.00 wt % and 73.38 wt %, respectively, with small amounts of Fe_2O_3 (0.63 wt %–0.90 wt %) and SiO_2 (0.19 wt %–1.72 wt %) (Table 1). This composition is similar to that of spinel ($MgAl_2O_4$) with an allochromatic colour mainly due to the substitution of aluminium (Al^{3+}) by chromium (Cr^{3+}) (Fritsch and Rossman, 1987; Giuliani et al., 2017).

The only analysed turquoise sample shows high values of P_2O_5 (32.88 wt %), Al_2O_3 (36.92 wt %), CuO (8.23 wt %), and H_2O (17.53 wt %) (Table 1), in good agreement with the ideal composition of this mineral, $CuAl_6(PO_4)_4(OH)_8.4H_2O$. Small amounts of SiO_2 (1.86 wt %) and Fe_2O_3 (0.59 wt %) were also detected. The idiochromatic sky blue colour of this gemstone is due to the high content of divalent copper (Cu^{2+}) in the structure of the mineral, as well as by the low amount of iron giving greenish hues (Khorassani and Abedini, 1976; Fritsch and Rossman, 1987).

Pearls contain approximately 95 wt %–97 wt % CaO with significant amounts of MnO (0.08 wt %–0.14 wt %) and SrO (0.06 wt %–0.14 wt %) (Table 1), in good agreement with an aragonite composition. This mineral is the main constituent of a large majority of gem-quality pearls sometimes associated with small areas of another polymorph such as calcite and/or vaterite (Karampelas et al., 2019).

All chemical analyses by pXRF confirm the mineral identifications realized by Raman spectroscopy. Gemstones observed on the reliquary crown are therefore sapphire, emerald, spinel, almandine garnet, turquoise, and "pearl". The analyses of noble metals (Table 2) indicate that the filigrees and the plates constituting the crown contain 85 wt %–86 wt % Au, 6 wt %–8 wt % Ag, and 7 wt % Cu, thus confirming their relatively pure gold composition.

5 Discussion

5.1 Evolution of cutting techniques

The polishing of stones dates back to the 10th millennium BCE. From the 4th century BCE, technical improvements allowed smaller samples to be polished, thus spreading the cabochon cutting all around the world. This method gives nice colours to the gemstones and allows them to keep a maximal amount of material. In Europe, simple faceting, with a large table surrounded by four facets, has been known since the Middle Ages, but starting from the 14th century, more complex faceting methods progressively appeared (Bariand and Poirot, 1998; Brose, 1954; Klein, 2005).

The gemstones decorating the reliquary crown of Namur are characterized by various sizes and shapes (see results), sometimes with growth structures parallel to the crystal faces of the mineral (Fig. 2c). They were cut in cabochon (Fig. 2), the simplest method, without any polishing traces. Only one larger sapphire shows a large table with four surrounding facets (p5-2, Fig. 1a). These observations might suggest that all gemstones could be contemporary with the crown (beginning of the 13th century) or a little bit older, considering the simple cutting techniques used. However, these gemstones

could not be of extremely old manufacture because they are of small sizes and do not show marked polishing traces.

5.2 Geographic origin of gemstones and pearls

5.2.1 Emerald

Since ancient times, emerald has been a very popular gemstone, a symbol of power and eternity, thus explaining its intense trading. Historical samples were mined in three main localities: Swat Valley in Pakistan (unknown date before common era to 1958), Habachtal in Austria (500 BCE to 300 CE), and along the Nugrus Thrust in Egypt (e.g. Wadi Sikait) (3000 BCE to 1500 CE). In the 16th and 18th centuries CE, new emeralds of gem quality were discovered in Colombia and in Afghanistan (Panjshir Valley), respectively (Giuliani et al., 2000; Harrell, 2004; Aurisicchio et al., 2018). Generally, the emerald crystallization is due to metasomatic processes occurring in various geological contexts and involving fluids mobilizing different elements like Cr, V, and Be (Aurisicchio et al., 2018; Giuliani et al., 2019).

Chemical analyses of emeralds from several historical deposits in Pakistan, Austria, Egypt, and Afghanistan (Groat et al., 2008; Aurisicchio et al., 2018) have been compared with emeralds decorating the reliquary crown of Namur; however, emeralds from Colombia were omitted because America was not yet discovered in the 13th century. The ternary Cr_2O_3–V_2O_5–FeO diagram (Fig. 4a), as well as the chromium–vanadium diagram (Fig. 4b), show that the trace-element compositions of these samples are very close to those of emeralds from Pakistan, and more precisely from the Swat Valley or Khaltaro. A further study of inclusions and ^{18}O / ^{16}O isotopes would help us to choose between the two localities (Giuliani et al., 2019). The good to excellent quality of the stones, as well as their dark green colour due to the high amounts of chromium, would also confirm this assumption (Gübelin, 1982); Egyptian samples are of poorer quality (Harrell, 2004).

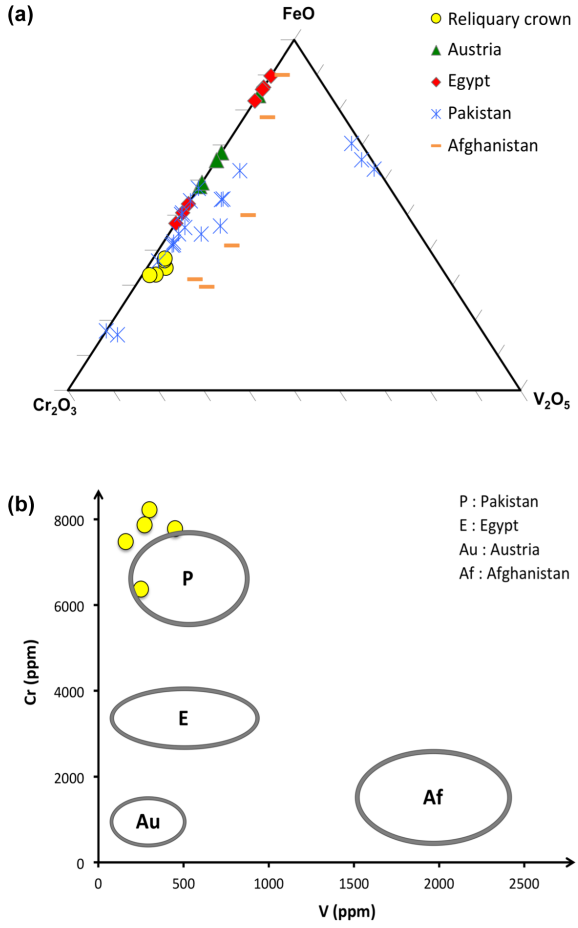

Figure 4. Chemical compositions of emerald from the reliquary crown of Namur compared to those of emerald from various localities. The ternary Cr_2O_3–V_2O_5–FeO diagram **(a)**, as well as the chromium-vanadium diagram **(b)**, were established by Groat et al. (2008) and Aurisicchio et al. (2018).

5.2.2 Garnet

Garnet popularity increased between the Egyptian Predynastic Period (3000 BCE) and the Early Middle Ages (600 CE) to become one of the most common gemstones. At that time, India was the dominant producer, but from the 7th century, Indian garnets were progressively replaced by Bohemian pyropes because of supply difficulties partly due to geopolitical conflicts (Calligaro et al., 2007; Thoresen and Schmetzer, 2013; Calligaro and Périn, 2019). However, the trade connection between India and the Mediterranean region still existed in the 13th century (Abu-Lughod, 1990).

On the basis of the Ca and Mg contents of garnets from various localities, Calligaro et al. (2007) and Gilg et al. (2010) identified five "types" or six "clusters" of samples (Fig. 5a): type I (= cluster B) and type II (= cluster A) correspond to almandine from different deposits in India; type III (= cluster X) corresponds to pyrope ("rhodolite" variety) from Sri Lanka (Ceylon); type IV (= cluster D) and type V (= cluster E) correspond to pyrope with or without chromium occurring in Portugal and Bohemia, respectively; cluster C corresponds to Scandinavian garnets.

According to the chemical analyses (Table 1), garnets decorating the reliquary crown of Namur show very low CaO (0.48 wt %–2.00 wt %) and MgO contents (3 wt %–7 wt %), thus corresponding to almandine of types I and II (Fig. 5a), certainly from an Indian source. The Fe_{tot} vs. CaO diagram, established by Greiff (1999) from many Asian almandine compositions, confirm this origin, and the MnO vs. FeO diagram allows us to identify three well-defined regions in India: Rajasthan, Madhya Pradesh, and Andhra Pradesh (Fig. 5b). Rajasthan is indeed one of the most productive garnet sources in the world, still providing many gem-quality samples nowadays. India is therefore a plausible origin for

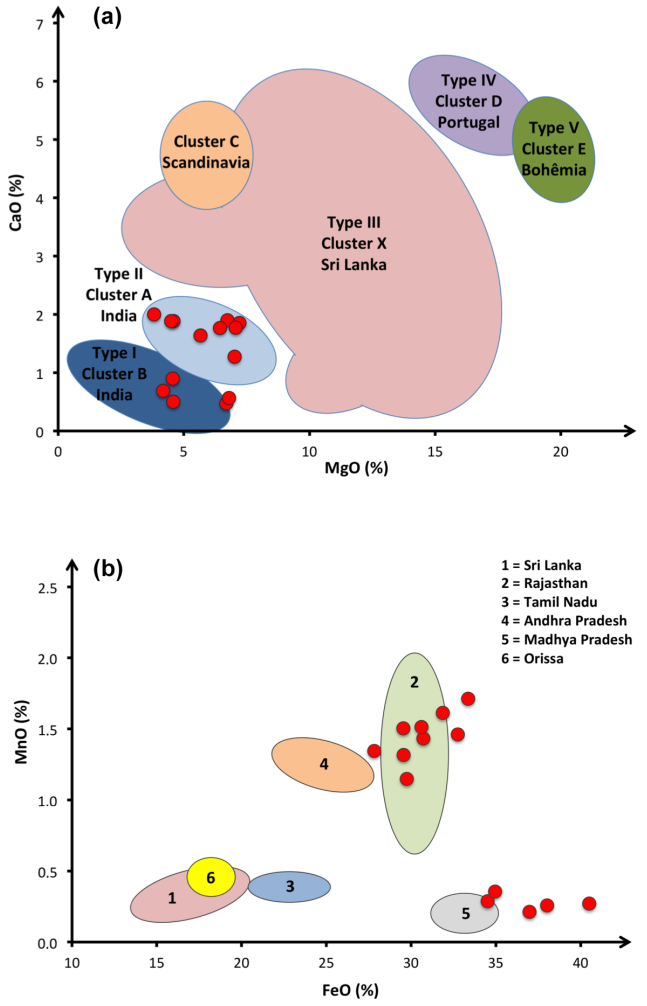

Figure 5. Compositional variations of garnet from several localities. The red dots represent the samples from the reliquary crown of Namur plotted in the CaO vs. MgO diagram published by Calligaro et al. (2007) and Gilg et al. (2010) **(a)**, as well as in the MnO vs. FeO diagram established by Greiff (1999) **(b)**.

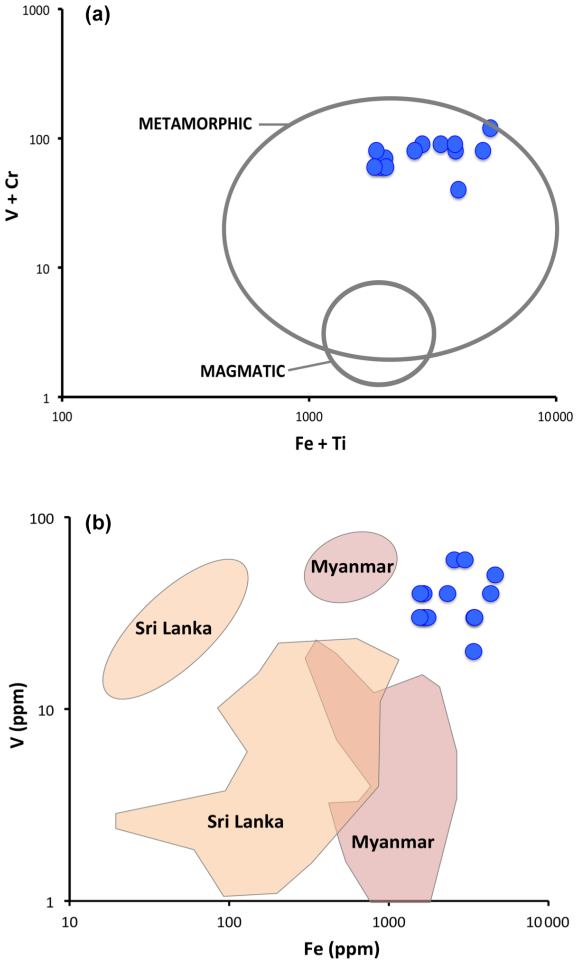

Figure 6. Chemical compositions of sapphire from the reliquary crown of Namur plotted in the (V + Cr) vs. (Fe + Ti) diagram established by Sutherland et al. (2015) and Chulapakorn et al. (2014) **(a)**, as well as in the Fe vs. V diagram published by Atikarnsakul et al. (2018) **(b)**.

these large-size gem almandines (Fig. 2b, h) because similar quality deposits are relatively rare, excluding a few European mines producing lower-quality stones. However, almandine is a common mineral with plenty of consumed or lost deposits around the world (Calligaro et al., 2007; Calligaro and Périn, 2019).

5.2.3 Sapphire

Traditional sources for the world's best-quality blue sapphires are located in North India (Kashmir), Myanmar, and Sri Lanka. This gemstone, also mined in Thailand, Australia, Madagascar, and Vietnam, crystallizes in magmatic or metamorphic environments impoverished in silica and enriched in alumina, iron, and titanium (Simonet et al., 2008; Shor and Weldon, 2009; Giuliani et al., 2014). Myanmarese (Mogok) and Sri Lankan deposits had been discovered approximately by the beginning of the Middle Ages, while the other deposits are dated from the 15th century for Thailand, from the 19th century for Kashmir, and from the late 20th century for Australia, Madagascar, and Vietnam (Shor and Weldon, 2009; Lucas et al., 2014; Saeseaw et al., 2017). According to Sutherland et al. (2015) (Fig. 6a) and Chulapakorn et al. (2014), the (V + Cr) vs. (Fe + Ti) plot, as well as the high Ti content (> 300 ppm) and low Fe amount (< 4200 ppm), show that all sapphires analysed have a metamorphic origin, thus indicating Sri Lankan or Myanmarese deposits (Lucas et al., 2014; Sutherland et al., 2015; Pehrson, 2017). The Fe vs. V diagram published by Atikarnsakul et al. (2018) does not allow us to choose between these two sources (Fig. 6b); however, the relatively high Fe content makes Sri Lanka an unlikely origin.

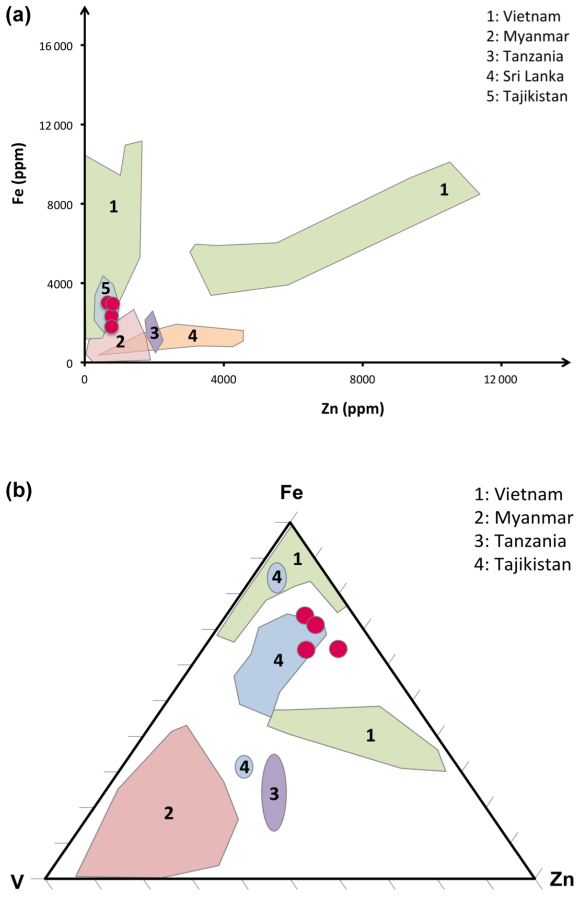

Figure 7. Chemical analyses of spinel from the reliquary crown of Namur plotted in the Fe vs. Zn **(a)** and Fe–Zn-V **(b)** diagrams published by Giuliani et al. (2017).

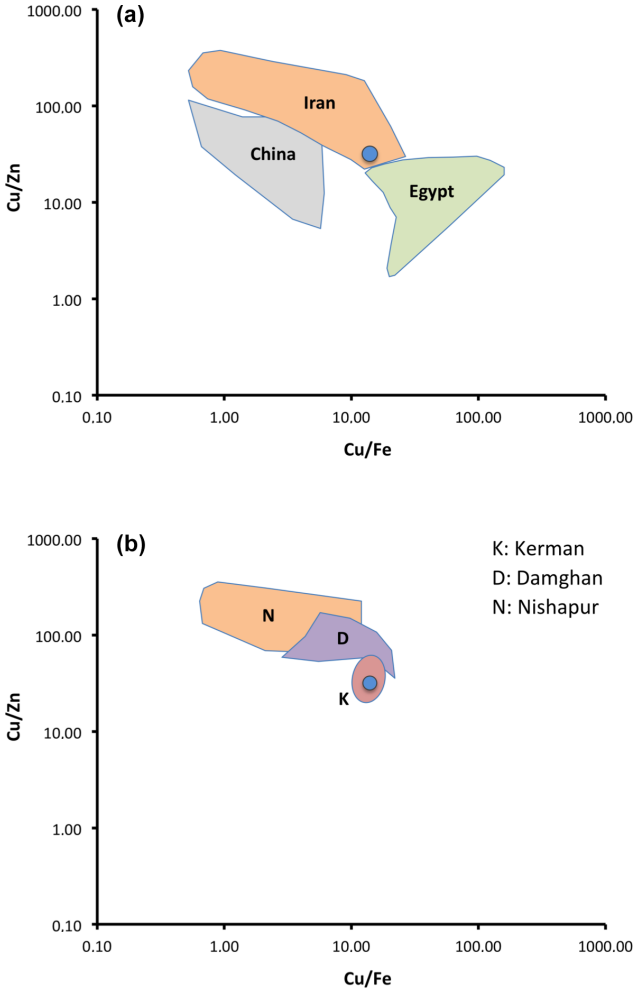

Figure 8. Cu / Zn vs. Cu / Fe diagrams established by Carò et al. (2017) in which the chemical compositions of turquoise from the reliquary crown of Namur are plotted.

Visually, sapphires adorning the crown mainly show an intense to saturated blue colour depending on Fe–Ti concentrations (Table 1) and sometimes with few small inclusions, star structures (Fig. 2d), or growth bands (Fig. 2c). Mogok deposits show sapphires that may exceed 100 carats and show a light to saturated blue colour with many inclusions, occasionally forming fine stars (Atikarnsakul et al., 2018), while Sri Lankan deposits, essentially situated in the highland complex, are famous for their large, gem-quality, and relatively poor-in-inclusion samples, as well as for their star sapphires (Zwaan, 1982; Lucas et al., 2014; Pehrson, 2017). Sri Lanka was also the first country to export this gemstone to Europe (Shor and Weldon, 2009). Therefore, both visual and chemical distinctions between sapphires from the two deposits are very difficult without using microscopic inclusion observations or more invasive techniques to analyse inclusions or to detect trace elements such as gallium.

5.2.4 Spinel

Nowadays, red to pink gem spinels are found in five majors deposits situated in Tanzania, Myanmar, Vietnam, Sri Lanka, and Tajikistan (Krzemnicki, 2010; Giuliani et al., 2017). They occur mainly in marbles affected by high-temperature metamorphism. During the Middle Ages, only two deposits were already mined, namely Kuh-i-Lal in Tajikistan and Mogok in Myanmar. At that time, spinels, often confused with rubies, were called "ruby spinel" or "balas ruby", in reference to Balascia (now Badakhshan) in Afghanistan (Malsy and Klemm, 2010; Giuliani et al., 2017; Pardieu and Farkhodova, 2019).

Giuliani et al. (2017) have published a Fe vs. Zn diagram to compare spinels from Sri Lanka, Vietnam, Myanmar, Tanzania, and Tajikistan. The samples decorating the reliquary crown of Namur show compositions very close to those of spinels from Tajikistan, without being able to exclude Myanmar and Vietnam (Fig. 7a). This last source is, however, impossible because the Luc Yen mine was only discovered during the end of the 20th century (Van Long et al., 2013). The Fe–V–Zn ternary plot, also published by Giuliani

et al. (2017), compares spinels from the same localities except Sri Lanka. As shown in Fig. 7b, samples from the reliquary crown are close to those of Tajikistan and Vietnam but far from those of Myanmar. The historical mine of Kuh-i-Lal, renown for producing exceptional gem-quality, red to pink (mostly) spinels which crystallized in high-temperature marbles during the formation of the Himalayan mountain belt (Malsy and Klemm, 2010; Giuliani et al., 2017; Pardieu and Farkhodova, 2019), is consequently the probable source for our samples.

5.2.5 Turquoise

Turquoise primary deposits, known since approximately the 4th millennium BCE, are situated in Egypt (Sinai), Iran (Nishapur, Kerman, and Damghan), and Central Asia (Uzbekistan and Afghanistan area). The sky-blue samples, considered as the finest, occur mainly in Nishapur, Iran (Wodiska, 1909; Khorassani and Abedini, 1976; Carò et al., 2017; Ovissi et al., 2017). Chinese mines, currently the most productive along with those of the United States, were only discovered during the 20th century (Chen et al., 2012). In Europe, turquoise samples are very rarely marketable as gems due to their greenish hue and porous aspect; the finest stones were consequently imported from Iran (Pogue, 1915; Ovissi et al., 2017).

Turquoise samples on the reliquary crown of Namur show a sky-blue colouration and an Fe_2O_3 content lower than 0.6 wt % (Table 1). Such low iron contents are typical for skye-blue turquoise, as underlined by Khorassani and Abedini (1976). To compare Chinese, Egyptian, and Iranian turquoise, Carò et al. (2017) have published two plots: Cu / Zn vs. Cu / Fe (Fig. 8a) and Cu / Zn vs. Cu / As. In both diagrams, our samples are included in the Iranian zone, thus confirming that gem-quality European turquoises were imported from Iran in the Middle Ages (Khorassani and Abedini, 1976; Ovissi et al., 2017). With the same diagram, Carò et al. (2017) also compared different localities in Iran, namely Nishapur, Kerman, and Damghan. Turquoise samples from the crown of Namur show compositions close to those of turquoise from the Kerman zone (Fig. 8b), but Central Asian samples do not appear in the diagram due to the lack of reference specimens from that region (Carò et al., 2017).

5.2.6 Pearls

Natural pearls were very popular during the Middle Ages, representing approximately 75 % of the gem trade. The process for making cultured pearls was developed at the end of the 19th century (Nagai, 2013), so it is theoretically impossible to find this kind of pearl on the reliquary crown. Generally, natural pearls found in the Middle East (e.g. Indian Ocean and Persian Gulf) are rounded with a shiny lustre and are slightly coloured, and they were mainly collected in saltwater. In contrast, European pearls (e.g. France and Scotland) are generally smaller, less transparent, and less shiny, and they were often collected in freshwater rivers. Due to their poorer quality, European pearls were therefore cheaper, less prestigious, and mainly used for decorating ecclesiastic items (Kunz and Stevenson, 1908; Amar and Lev, 2017; Karampelas et al., 2019).

The distinction between saltwater and freshwater pearls is possible from their amounts of manganese and strontium: Sr is higher (2000 to 3000 ppm) and Mn lower (0.5 to 10 ppm) in saltwater pearls, while it is the contrary for freshwater pearls (100 to 1500 ppm Sr and 100 to 8000 ppm Mn) (Habermann et al., 2001; Wehrmeister et al., 2007). According to the Mn vs. Sr diagram published by Wehrmeister et al. (2007), pearls decorating the crown of Namur have a freshwater origin since they show low Sr concentrations between 290 and 620 ppm, as well as high Mn concentrations between 330 and 600 ppm. Consequently, given the variations in quality, size, and shape, these natural freshwater pearls are certainly from several rivers in Europe, maybe from Scotland for the lower-quality pearls and from France for the best samples (Gontero-Lauze, 2012). The exact origin of the pearls investigated here is impossible to determine since trace-element analyses only allow for the determination of saltwater vs. freshwater origin. Moreover, several pearls are pierced in their centre (Fig. 1a and c), certainly indicating a recovery from older items, as for example necklaces or bracelets.

5.3 Gemstone trading in the Middle Ages

The gemstones decorating the crown of Namur are sapphire, emerald, spinel, almandine garnet, turquoise, and "pearls". During the Middle Ages, the best-quality samples of these gemstones were mainly imported from the Middle East, particularly from India, Sri Lanka, Thailand, Vietnam, and Myanmar (Calligaro et al., 2007; Aurisicchio et al., 2018).

Between the 10th and the 13th centuries, two major trade roads existed between Europe and Asia. The first one, named the "silk road", started in China, transited through Central Asia or North India, and generally reached European countries via Italy (Rome) or Turkey (Constantinople/Istanbul). Spinels from Tajikistan, as well as emeralds from Pakistan, were imported along this famous road (Sevillano-López and González, 2011; Pardieu and Farkhodova, 2019). The second road used the Indian Ocean to link India and Sri Lanka to the Mediterranean Basin, passing through Egypt (Abu-Lughod, 1990; Sevillano-López and González, 2011; Lucas et al., 2014).

According to Collet (2013), the gemstones decorating the reliquary crown of Namur would be contemporaneous with the two holy thorns and originate from Constantinople, or they would be recovered from various ancient Namur goldsmithery items. The first hypothesis seems the most likely because, for each kind of gem, the pXRF analyses are quite

similar, indicating a unique source. This hypothesis is further confirmed by the fact that Constantinople was a famous gem trade centre on the silk road during the Middle Ages (Sevillano-López and González, 2011).

6 Conclusion

The reliquary crown of Namur, dated to the beginning of the 13th century, is decorated by ca. 400 gemstones, comprising blue sapphires, emeralds, reddish pink spinels, red almandine garnets, turquoises, and "pearls" with simple cuttings. The filigrees contain approximately 86 wt % Au, 7 wt % Ag, and 7 wt % Cu, thus confirming their relatively pure gold composition. Sapphires were imported from Sri Lanka or Myanmar, emeralds from Pakistan, spinels from Tajikistan, turquoises from Iran, garnets from India, and pearls from different European deposits. The gemstones, contemporary with the crown, probably arrived in Europe by the silk trade road. The archaeometric investigation of religious goldsmith artwork with non-destructive techniques like pXRF or Raman spectrometry is a necessary step to better understand the historical and geographic contexts in which these objects were produced.

Data availability. All data are available upon request to Yannick Bruni.

Supplement. The supplement related to this article is available online at: https://doi.org/10.5194/ejm-33-221-2021-supplement.

Author contributions. This work is part of the PhD project of YB, who analysed the crown of Namur with FH. HC provided access to the crown and gave us the historical background for this reliquary. PG improved the historical background, and DS loaned the Raman spectrometer and helped us to write the experimental methods. The pXRF was loaned by the Laboratory of Mineralogy of the Liège University (FH). The text was written by YB and corrected by FH.

Competing interests. The authors declare that they have no conflict of interest.

Acknowledgements. Nicolas Delmelle is acknowledged for his help during the Raman and pXRF analyses. We also thank Hélène Cambier, curator of the treasure of Namur and the diocesan museum, for the authorization to analyse the crown and help in its handling.

Review statement. This paper was edited by Reto Gieré and reviewed by two anonymous referees.

References

Abu-Lughod, J. L.: Before European hegemony: The World System, A.D., 1250–1350, The business History Rev., 64, 362–364, 1990.

Amar, Z. and Lev, E.: Most-Cherished Gemstones in the Medieval Arab World, J. Royal Asiatic Soc., Series 3, 27, 377–401, 2017.

Athavale, S. A. and Hambarde, M. S.: Raman scattering: Fingersprint for Identification of nature and color origin of Pearls, Int. Res. J. Eng. Technol. (IRJET), 7, 2065–2078, 2020.

Atikarnsakul, U., Vertriest, W., and Soonthorntantikul, W.: Characterization of blue sapphires from the Mogok stone tract, Mandalay region, Burma (Myanmar), GIA News from Research, Special Issue, 1–56, 2018.

Aurisicchio, C., Conte, A. M., Medeghini, L., Ottolini, L., and De Vito, C.: Major and trace element geochemistry of emerald from several deposit: Implications for genetic models and classification schemes, Ore Geol. Rev., 94, 351–366, 2018.

Bariand, P. and Poirot, J.-P.: Larousse des pierres précieuses, Larousse-Bordas, Paris, 288 pp., 1998.

Brose, H. W.: A Short History of Faceting, Lapidary J., 2, 446–452, 1954.

Bruni, Y., Hatert, F., George, P., and Strivay, D.: The Reliquary bust of Saint Lambert from the Liège cathedral, Belgium: gemstones and glass beads analysis by pXRF and Raman spectroscopy, Archaeometry, 62, 297–313, 2019.

Bruni, Y., Hatert, F., George, P., and Strivay, D.: An archaeometric investigation of glass beads decorating the reliquary of Saint Simètre from Lierneux, Belgium, J. Archaeol. Sci. Report, 32, 1–6, 2020.

Calligaro, T., Périn, P., Vallet, F., and Poirot, J-P.: Contribution à l'étude des grenats mérovingiens (Basilique de Saint-Denis et autres collections du musée d'Archéologie nationale, diverses collections publiques et objets de fouilles récents), Antiquités Nationales, 38, 111–144, 2007.

Calligaro, T. and Périn, P.: Le commerce des grenats à l'époque mérovingienne, Archéopages, HS 5, 109–120, 2019.

Carò, F., Schorsch, D., and Santarelli, B.: Proveniencing Turquoise Artifacts from Ancient Egyptian Contexts: A Non-invasive XRF Approach, Sci. of Anc. Egypt. Mat. and Tech. (SAEMT) conference, Abstract book, 2017.

Chen, Q., Yin, Z., Qi, L., and Xiong, Y.: Turquoise from Zhushan County, Hubei province, China, Gems Gemol., 48, 198–204, 2012.

Chulapakorn, T., Intarasiri, S., Bootkul, D., and Singkarat, S.: Identification of deposit types of natural corundum by PIXE, Nuclear Instruments and Methods in Physics Research, B331, 108–112, 2014.

Collet, E.: Trésors classés de la Cathédrale de Namur, Fondation roi Baudouin, Belgium, 40 pp., 2013.

Culka, A. and Jehlička, J.: A database of Raman spectra of precious gemstones and minerals used as cut gems obtained using portable sequentially shifted excitation Raman spectrometer, J. Raman Spectrosc., 50, 262–280, 2019.

Demaude, M.: Etude gemmologique de pièces d'orfèvrerie du Trésor de la Cathédrale Saint-Paul de Liège, Master thesis, University of Liège, 81 pp., 2016.

Demaude, M., Bruni, Y., Hatert, F., and Strivay, D.: Étude gemmologique de la croix-reliquaire à double traverse du Trésor de

la Cathédrale de Liège, Trésor de Liège, Bulletin trimestriel, 50, 9–15, 2017.

Ferreira de Araújo Neto, J., de Brito Barreto, S., Andressa Carrino, T., Müller, A., and Montefalco de Lira Santos, L. C.: Mineralogical and gemological characterization of emerald crystals from Paraná deposit, NE Brazil: a study of mineral chemistry, absorption and reflectance spectroscopy and thermal analysis, Brazilian J. Geol., 49, 1–15, 2019.

Fritsch, E. and Rossman, G. R.: An update on color in gems. Part1: Introduction and colors caused by dispersed metal ions, Gems Gemol., 23, 126–139, 1987.

Fritsch, E. and Rossman, G. R.: An update on color in gems. Part2: Colors involving multiple atoms and colors centers, Gems Gemol., 24, 3–15, 1988.

Gaborit-Chopin, D.: Les couronnes du sacre des rois et des reines au trésor de Saint-Denis, Bull. Monumental, 133, 165–174, 1975.

Gilg, H. A., Gast, N., and Calligaro, T.: Vom Karfunkelstein, Archäologische Staatssammlung, 37, 87–100, 2010.

Giuliani, G., Chaussidon, M., Schubnel, H.-J., Piat, D. H., Rollion-Bard, C., France-Lanord, C., Giard, D., de Narvaez, D., and Rondeau, B.: Oxygen Isotopes and Emerald Trade Routes since Antiquity, Sciences, 287, 631–633, 2000.

Giuliani, G., Ohnenstetter, D., Fallick, A. E., Groat, L., and Fagan, A.,J.: The geology and genesis of gem corundum deposits, Mineral. Assoc. Canada Short Course, 44, 29–112, 2014.

Giuliani, G., Fallick, A. E., Boyce, J., Pardieu, V., and Pham, V.-L.: Pink and red Spinels in marble: Trace elements, Oxygen isotopes, and Sources, Can. Mineral., 55, 743–761, 2017.

Giuliani, G., Groat, L. A., Marshall, D., Fallick, A. E., and Branquet, Y.: Emerald Deposits: A Review and Enhanced Classification, Minerals, 9, 1–63, 2019.

Gontero-Lauze, V: Les pierres du Moyen Age, Les Belles Lettres, Paris, France, 222 pp., 2012

Greiff, S.: Naturwissenschaftliche Untersuchungen zur Frage der Rohsteinquellen für frühmittelalterlichen Almandingranatschmuck rheinfränkischer Provenienz, Jahrb. Römisch-Germanischen Zentral Museums Mainz, 45, 599–645, 1999.

Groat, L. A., Giuliani, G., Marshall, D. D., and Turner, D.: Emerald deposits and occurrences: A review, Ore Geol. Rev., 34, 87–112, 2008.

Gübelin, E. J.: Gemstones of Pakistan: Emerald, Ruby, and Spinel, Gems Gemol., 18, 123–139, 1982.

Habermann, D., Banerjee, A., Meijer, J., and Stephan, A.: Investigation of manganese in salt- and freshwater pearls, Nuclear Instrum. Methods Phys. Res. B, 181, 739–743, 2001.

Harrell, J. A.: Archaeological Geology of the World's First Emerald Mine, Geosci. Canada, 31, 69–76, 2004.

Jehlička, J., Culka, A., Vandenabeele, P., and Edwards, H. G. M.: Critical evaluation of a handheld Raman spectrometer with near infrared (785 nm) excitation for field identification of minerals, Spectrochim. Acta, A80, 36–40, 2011.

Kadleíková, M., Breza, J., and Vesely, M.: Raman spectra of synthetic sapphire, Microelectronics J., 32, 955–958, 2001.

Karampelas, S., Fritsch, E., Makhlooq, F., Mohamed, F., and Al-Alawi, A.: Raman spectroscopy of natural and cultured pearls and pearl producing mollusc shells, J. Raman Spectrosc., Special Issue, 1–9, 2019.

Khorassani, A. and Abedini, M.: A new study of turquoise from Iran, Mineral. Mag., 40, 640–642, 1976.

Klein, G.: Faceting History: cutting diamonds & colored stones, Xlibris Corporation, USA, 242 pp., 2005.

Krzemnicki, M. S.: Spinel: A Gemstone on the rise, SSEF, Hong Kong conference, 27 pp., 2010.

Kunz, G. F. and Stevenson, C. H.: The book of the Pearl: The History, Art, Science, and Industry of the Queen of Gems, The Century Company, New York, USA, 552 pp., 1908.

Lucas, A., Sammoon, A., Jayarajah, A. P., Hsu, T., and Padua, P.: Sri Lanka: Expedition to the Island of jewels, Gems Gemol., 50, 1–59, 2014.

Malsy, A. and Klemm, L.: Distinction of Gem Spinels from the Himalayan Mountain Belt, Chimia, 64, 741–746, 2010.

Nagai, K.: A History of the Cultured Pearl Industry, Zool. Sci., 30, 783–793, 2013.

Ovissi, M., Yazdi, M., and Ghorbani, M.: Turquoise grading in Persian historical and modern times; a comparative study, 35th National Geosciences Conference of Geological Survey of Iran, Tehran, 19–21 February 2017, 1–6, 2017.

Pardieu, V. and Farkhodova, T.: Spinel from Tajikistan: The Gem that Made Famous the World "Ruby", InColor Magazine, Special Spinel, 43, 30–33, 2019.

Pehrson, E. A. K.: Identification methods of Sri Lanka corundum in comparison to other common gemstones, Uppsala University, Department of Earth Sciences, 5, 1–32, 2017.

Pogue, J. E.: The turquoise: A study of its History, Mineralogy, Geology, Ethnology, Archaeology, Mythology, Folklore and Technology, Memoirs of the National Academy of Sciences, Cornell University Library, USA, 12, 642 pp., 1915.

RRUFF: Integrated Database of Raman Spectra, available at: http://rruff.info/ (last access: 5 January 2021), 2020.

Saeseaw, S., Sangsawong, S., Vertriest, W., Atikarnsakul, U., Raynaud-Flattot, L. V., Khowpong, C., and Weeramonkhonlert, V.: A study of sapphire from Chanthaburi, Thailand and its gemological characteristics, GIA News from Research, Special Issue, 1–42, 2017.

Salet, F.: La chasse des Saints-Innocents au trésor de la cathédrale de Cologne, Bull. Monumental, 125, 311–312, 1967.

Sevillano-López, D. and González F. J.: Mining and Minerals trade on the silk road to the ancient literary sources: 2 BC to 10 AD centuries, in: History of Research in Mineral Resources, edited by: Ortiz, J. E., Puche, O., Rábano, I., and Mazadiego, L. F., Cuadernos del Museo Geominero, Instituto Geológico y Minero de España, Madrid, Spain, 13, 43–53, 2011.

Shor, R. and Weldon, R.: Ruby and sapphire production and distribution: A quarter century of change, Gems Gemol., 45, 236–259, 2009.

Simonet, C., Fritsch, E., and Lasnier, B.: A classification of gem corundum deposits aimed towards gem exploration, Ore Geol. Rev., 34, 127–133, 2008.

Sutherland, F. L., Zaw, K., Meffre, S., Yui, T.-F., and Thu, K.: Advances in trace element "Fingerprinting" of gem corundum, ruby and sapphire, Mogok area, Myanmar, Minerals, 5, 61–79, 2015.

Thoresen, L. and Schmetzer, K.: Greek, Etruscan and Roman garnets in the antiquities collection of the J. Paul Getty Museum, J. Gemmol., 33, 201–222, 2013.

Van Long, P., Pardieu, V., and Giuliani, G.: Update on Gemstone Mining in Luc Yen, Vietnam, Gems Gemol., 49, 233–245, 2013.

Vanrillaer, L.: Un écrin sous-estimé au sein du Trésor de la cathédrale Saint-Aubin de Namur: le coffret des Saintes Épines, Anal-

yses techniques, morphologiques et iconographiques accompagnées d'une typologie des coffrets, Mémoire de Master, Faculté de philosophie, arts et lettres, Université catholique de Louvain, 2017.

Van Tricht, F.: La gloire de l'empire : l'idée impériale de Henri de Flandre-Hainaut, deuxième empereur latin de Constantinople (1206–1216), Byzantion, 70, 211–241, 2000.

Wehrmeister, U., Jacob, D. E., Soldati, A. L., Hager, T., and Hofmeister, W.: Vaterite in freshwater cultured pearls from China and Japan, J. Gemmol., 31, 269–276, 2007.

Wodiska, J.: A Book of Precious Stones: The identification of gems and minerals, and an account of their scientific, commercial, artistic, and historical aspects, Putnam, New-York, USA, 370 pp., 1909.

Zwaan, P. C.: Sri Lanka: The gem island, Gems Gemol., 18, 62–71, 1982.